Dr. A. P. J. Abdul Kalam Government College

Department of Chemistry

ONLINE STUDY RESOURCE

For Detailed Discussion Contact Any Faculty Member Electronically

5
Surface tension

At the interface between two materials physical properties change rapidly over distances comparable to the molecular separation scale. Since a molecule at the interface is exposed to a different environment than inside the material, it will also have a different binding energy. In the continuum limit where the transition layer becomes a mathematical surface separating one material from the other, the difference in molecular binding energy manifests itself as a macroscopic *surface energy density*. And where energy is found, forces are not far away.

Molecules sitting at a free liquid surface against vacuum or gas have weaker binding than molecules in the bulk. The missing (negative) binding energy can therefore be viewed as a positive energy added to the surface itself. Since a larger area of the surface contains larger surface energy, external forces must perform positive work against internal surface forces to increase the total area of the surface. Mathematically, the internal surface forces are represented by *surface tension*, defined as the normal force per unit of length. This is quite analogous to bulk tension (i.e. negative pressure), defined as the normal force per unit of area.

In homogeneous matter such as water, surface tension does not depend on how much the surface is already stretched, but stays always the same. Certain impurities, called *surfactants*, have dramatic influence on surface tension because they agglomerate on the surface and form an elastic skin which resists stretching with increasing force. Best known among these are soaps and detergents from which one can blow so beautiful bubbles. A lipid membrane also surrounds every living cell and separates the internal biochemistry from the outside.

Although surface tension is present at all interfaces, it is most important for small fluid bodies. At length scales where surface tension does come into play the shape of an interface bears little relation to the gravitational equipotential surfaces that dominate the static shapes of large-scale systems analyzed in the preceding chapter. In this chapter surface tension is introduced and only applied to various hydrostatic systems. The physics of surface tension has a long history and excellent books exist on this subject, for example the recent [Gennes et al. 2002].

5.1 Basic physics of surface tension

Although surface tension may be taken as a primary phenomenological concept in continuum physics, it is nevertheless instructive first to make a simple molecular model which captures the essential features of the phenomenon and even allows us to make an estimate of its magnitude. Afterwards we shall define the concept without recourse to molecules.

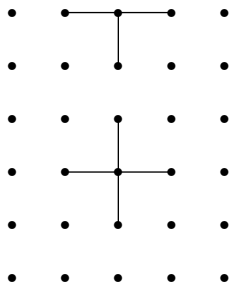

Cross section of a primitive three-dimensional model of a material interfacing to vacuum. A molecule at the surface has only five bonds compared to the six that link a molecule in the interior. The missing bond energy at the surface gives rise to a positive surface energy density, which is the cause of surface tension.

Molecular origin of surface energy

Even if surface tension is most important for liquids, we shall here consider a simple regular "solid" surrounded by vacuum. The molecules are placed in a cubic grid (see the margin figure) with grid length equal to the molecular separation length L_{mol}. Each molecule in the interior has six bonds to its neighbors whereas a surface molecule has only five. If the total binding energy of a molecule in the bulk is ϵ, a surface molecule will only be bound by $\frac{5}{6}\epsilon$. The missing binding energy corresponds to adding an extra positive energy $\frac{1}{6}\epsilon$ for each surface molecule.

The binding energy may be estimated as $\epsilon \approx h\,m$ where h is the specific heat of evaporation (evaporation enthalpy per unit of mass) and $m = M_{\text{mol}}/N_A = \rho L_{\text{mol}}^3$ is the mass of a single molecule. Dividing the molecular surface energy $\frac{1}{6}\epsilon$ with the molecular area scale L_{mol}^2, we arrive at the following estimate of the surface energy density[1],

$$\alpha \approx \frac{\frac{1}{6}\epsilon}{L_{\text{mol}}^2} \approx \frac{1}{6}\,\frac{hm}{L_{\text{mol}}^2} \approx \frac{1}{6}\,h\,\rho\,L_{\text{mol}}. \tag{5.1}$$

The appearance of the molecular separation scale is quite understandable because ρL_{mol} represents the effective surface mass density of a layer of thickness L_{mol}. One might expect that the smallness of the molecular scale would make the surface energy density insignificant in practice, but the small thickness is offset by the fairly large values of ρ and h in normal liquids, for example water.

	α[mJ m^{-2}]	est
Water	72	126
Methanol	22	62
Ethanol	22	55
Bromine	41	44
Mercury	337	222

Surface energy (or surface tension) for some liquids at 25° C in units of millijoule per square meter. The estimates are obtained using eq. (5.1) . Data from [Lide 1996].

In the margin table a few measured and estimated values are shown. For water the mass density is $\rho \approx 10^3$ kg m^{-3} and the specific evaporation heat $h \approx 2.4 \times 10^6$ J kg^{-1}, leading to the estimate $\alpha \approx 0.126$ J m^{-2}, which should be compared to the measured value of 0.072 J m^{-2} at 25° C. Although not impressive these estimates are not too bad, considering the crudeness of the model.

Work and surface energy density

Increasing the area of an interface with energy density α by a tiny amount dA requires an amount of work equal to the surface energy contained in the extra piece of interface,

$$\boxed{dW = \alpha\,dA.} \tag{5.2}$$

Except for the sign, this is quite analogous to the mechanical work $dW = -p\,dV$ performed against bulk pressure when the volume of the system is expanded by dV. But where a volume expansion under positive pressure performs work *on* the environment, increasing the area against a positive surface energy density requires work *from* the environment.

The surface energy density associated with a liquid or solid interface against vacuum (or gas) is always positive because of the missing negative binding energy of the surface molecules. The positivity of the surface energy density guarantees that such interfaces seek towards the minimal area consistent with the other forces that may be at play, for example gravity. Small raindrops and air bubbles are for this reason nearly spherical. Larger falling raindrops are also shaped by viscous friction and air currents, giving them a more complicated shape (see figure 5.1).

Interfaces between solids and liquids or between liquids and liquids are not required to have positive interfacial energy density. The sign depends on the strength of the cohesive forces holding molecules of a material together compared to the strength of the adhesive forces between the opposing molecules of the interfacing materials. The interface between a solid and liquid is normally not deformable, and a negative interfacial energy density has

[1] There is no universally agreed-upon symbol for surface tension which variously denoted α, γ, σ, S, Υ and T.

no dramatic effect. If on the other hand the interfacial energy density between two liquids is negative, a large amount of energy can be released by maximizing the area of the interface. Folding it like crumpled paper, the two fluids are mixed thoroughly instead of being kept separate. Fluids that readily mix with each other, such as alcohol and water, may be viewed as having negative interfacial energy density, although the concept is not particularly well-defined in this case. Immiscible fluids like oil and water must on the other hand have positive interfacial energy density which makes them seek towards minimal interface area with maximal smoothness.

Since an interface has no macroscopic thickness, it may be viewed as being locally flat everywhere, implying that the surface energy density cannot depend on the curvature of the interface, but only on the properties of the interfacing materials. If these are homogeneous and isotropic—as they often are—the value of the energy density will be the same everywhere on the interface. In the following we shall focus on hydrostatics of homogeneous materials and assume that surface tension takes the same value everywhere on a static interface (with exception of soap films).

Force and surface tension

The resistance against extension of a free surface shows that the surface has an internal *surface tension* which we shall now see equals the surface energy density α. Suppose we wish to stretch the surface along a straight line of length L by a uniform amount ds (see the margin figure). Since the area is increased by $dA = Lds$, it takes an amount of work $dW = \alpha L ds$, from which we conclude that the force we apply orthogonally to the line is $\mathcal{F} = dW/ds = \alpha L$. In equilibrium, the applied normal force per unit of length, $\mathcal{F}/L = \alpha$, defines the internal surface tension α. Surface tension is thus identical to surface energy density, and is of course measured in the same unit, N m^{-1} = J m^{-2}.

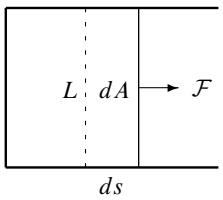

The basic surface tension experiment is a 2-dimensional version of the 3-dimensional experiment with a piston in a container. Using a soap film and metal wire as both 'container' and moveable 'piston', it can easily be carried out in the home.

Formally, surface tension is defined in much the same way as pressure was defined in equation (2.10) on page 24. Let an oriented open surface be divided into two parts by an oriented curve, such that the surface has a uniquely defined left and right hand side with respect to the curve. If $\hat{\boldsymbol{n}}$ denotes the normal to the surface, then

$$\boxed{d\boldsymbol{\mathcal{F}} = \alpha\, d\boldsymbol{\ell} \times \hat{\boldsymbol{n}},} \tag{5.3}$$

is the force that the right hand side of the surface exerts on the left hand side through the curve element $d\boldsymbol{\ell}$ (see the margin figure). The total force is obtained by integrating this expression along the curve. It follows immediately that to shift a piece of the curve of length L by ds orthogonal to the curve the work is given by eq. (5.2) with $dA = Lds$.

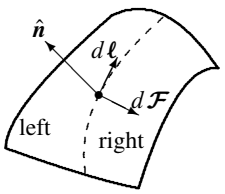

A piece of an oriented surface divided by an oriented curve (dashed). The cross product of the curve element $d\boldsymbol{\ell}$ and the surface normal $\hat{\boldsymbol{n}}$ determines the direction of the force with which the piece of the surface on the right acts on the piece on the left across the curve element.

At an interface between homogenous materials, surface tension does not depend on how much the interface has already been stretched, and this makes the interface quite different from an elastic membrane which like the skin of a balloon resists stretching with increasing force because elastic tension increases as the deformation grows (Hooke's law; see chapter 8). Soap films and biological membranes are an exception and behave like elastic membranes because of their peculiar surfactants. That is in fact what accounts for their great stability (see section 5.2).

Case: Pressure excess in a sphere

Everybody knows that the pressure inside a toy balloon is higher than outside, and that the excess pressure is connected with the tension in the taut balloon skin. Here we shall calculate the surface pressure discontinuity for a droplet of a homogeneous liquid hovering weightlessly, for example in a spacecraft. In the absence of all external forces, surface tension will attempt make the droplet spherical because that shape has smallest area for a given volume.

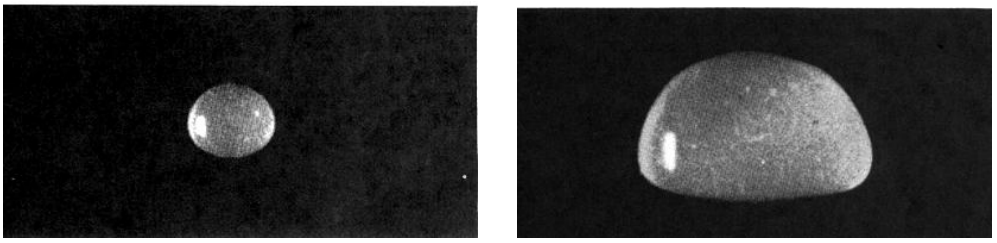

Figure 5.1. Steadily falling raindrops are subject to the combined effects of surface tension, gravity, friction, and air currents. **Left:** Small raindrops are dominated by surface tension and therefore nearly spherical. Here the drop radius is slightly larger than the capillary length of 2.7 mm and the drop is slightly oval. **Right:** Larger raindrops assume a typical "hamburger" shape. Reproduced from [McD54].

Surface tension will also attempt to contract the ball but is stopped by the build-up of an extra positive pressure Δp inside the liquid. If we increase the radius R by an amount dR we must perform the extra work $dW = \alpha\, dA - \Delta p\, dV$ where dA is the change in surface area and dV is the change in volume. Since $dA = d(4\pi R^2) = 8\pi R\, dR$ and $dV = d\left(\frac{4}{3}\pi R^3\right) = 4\pi R^2\, dR$, the work becomes $dW = (\alpha 8\pi R - \Delta p\, 4\pi R^2)\, dR$. In equilibrium, where the contraction forces must balance the pressure forces, there should be nothing to gain or lose, i.e. $dW = 0$, from which it follows that

$$\Delta p = \frac{2\alpha}{R}. \tag{5.4}$$

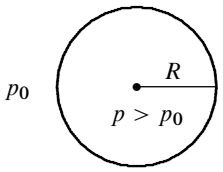

Surface tension makes the pressure higher inside a spherical droplet or bubble.

It should be emphasized that the above argument holds as well for a spherical air bubble in the same liquid: the pressure excess inside a bubble is exactly the same as in a droplet of the same radius.

A spherical raindrop of diameter 1 mm has an excess pressure of only about 300 Pa, which is tiny compared to atmospheric pressure (10^5 Pa). In clouds raindrops are tiny with diameter about 1 μm implying a pressure excess a thousand times larger, about 3 atm.

Capillary length

When can we disregard the influence of gravity on the shape of a raindrop? Consider a spherical raindrop of radius R falling steadily through the air with its weight being balanced by air drag. Since the drag force balances gravity, the condition must be that the variation in hydrostatic pressure inside the drop should be negligible compared to the pressure excess due to surface tension. We must in other words require that $\rho_0 g_0 2R \ll 2\alpha/R$ where ρ_0 is the density of water (minus the tiny density of air). Solving for R the inequality becomes $R \ll L_c$ where

$$L_c = \sqrt{\frac{\alpha}{\rho_0 g_0}} \tag{5.5}$$

The Danish Meteorological Institute (`http://www.dmi.dk`) uses the above symbol for heavy rain.

is the so-called *capillary length* (also called the *capillary constant*). For gravity to be negligible, the radius of the drop should be much smaller than the capillary length.

The capillary length equals 2.7 mm for the air–water interface at 25° C. Falling raindrops are deformed by the interaction with the air and never take the familiar teardrop shape with a pointed top and a rounded bottom, so often used in drawings—and even by some national meteorology offices. Small raindrops with radius up to about 2 mm are nearly perfect spheres, but for larger radius they become increasingly flattened (see figure 5.1). Eventually, when the radius exceeds 4.5 mm, a raindrop will break up into smaller drops due to the interaction with the air.

Although derived for a sphere, the capillary length is also the characteristic length scale at which static pending drops and captive bubbles begin to deviate from being spherical (see section 5.8). To understand how the capillary length, calculated from the density of water, can also be meaningful for an air bubble in water, one must remember that the surrounding water imposes a changing hydrostatic pressure over the bubble (which is the cause of buoyancy). More generally the density parameter should be taken to be $|\Delta\rho|$ where $\Delta\rho$ is the density difference between the fluid in the sphere and the fluid that surrounds it. When the two densities are nearly equal, the capillary length can become very large.

Marangoni forces

It is intuitively clear that any variation in surface tension along an interface will create tangential (shear) forces, so-called *Marangoni forces*. Such variation can arise from inhomogeneous material properties, or from temperature variations. Surface tension generally decreases with rising temperature which is one of the reasons we use hot water for washing ourselves and our clothes. Unless balanced by other forces shear surface forces cannot be sustained in a liquid at rest but will unavoidably set it into motion. In static soap bubbles gravity is in fact balanced by variations in surface tension caused by the elastic reaction to stretching of the bubble "skin". Apart from a discussion of this particular case in section 5.2, we shall not investigate the Marangoni effect and its consequences further here (see however [5]).

Carlo Guiseppe Matteo Marangoni (1840–1925). Italian physicist. Studied the effect of spatial variations in surface tension for his doctoral dissertation in 1865.

Soap-powered boat: The Marangoni effect has been exploited in toys, for example the soap-powered boat. The "boat" is made from a small piece of wood, polystyrene or cardboard cut out in a shape like the one in the margin figure. The "boat" is driven around on the water surface by a small piece of soap mounted at the rear end. The dissolving soap lowers the surface tension of the water behind the boat, and the unbalance with the larger surface tension ahead of the boat pulls the boat forward. The fun stops of course when the dissolving soap has reached the same concentration all over the water surface. A piece of camphor is also effective as motor for the little boat but is harder to come by.

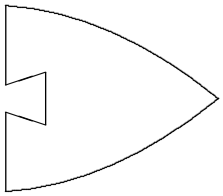

Shape of soap-powered boat. A pea-sized piece of soap or camphor is deposited in the small cut-out to the left.

5.2 Soap bubbles

Children and adults alike love to play with soap bubbles, and have done so for centuries [Boys 1959]. If you start to think a bit about what is really going on with these fantastic objects, many questions arise. Why do we need soap for making bubbles? Why can't one make bubbles out of pure water? How big can they become? How long can they last? Freely floating soap bubbles are fun because their weight (minus buoyancy) is so tiny that they remain floating in the slightest updraft. The skin of a soap bubble is so strong that a bubble can be supported by a hand or a wire frame as in figure 5.2 (right). Bubbles are not the only soap films that can be created. Using wire frames, it is possible to create all kinds of geometric shapes (see figure 5.3) that have attracted the lasting interest of mathematicians [CW06].

The nature of bubble liquid

An air-filled bubble created from a thin liquid film has always a huge surface area compared to the area of a spherical volume containing the same amount of liquid. Any external "agent" — gravity, drafts of air, encounters with other objects, evaporation, and draining — will stretch the skin in some places and maybe compress it in others. If the surface tension is constant, as it is for homogenous liquids like pure water, the same force will keep on stretching the skin until it becomes so thin that the bubble bursts, and instantly turns into one or more spherical droplets. Large air-filled bubbles with a skin made from pure water are inherently unstable.

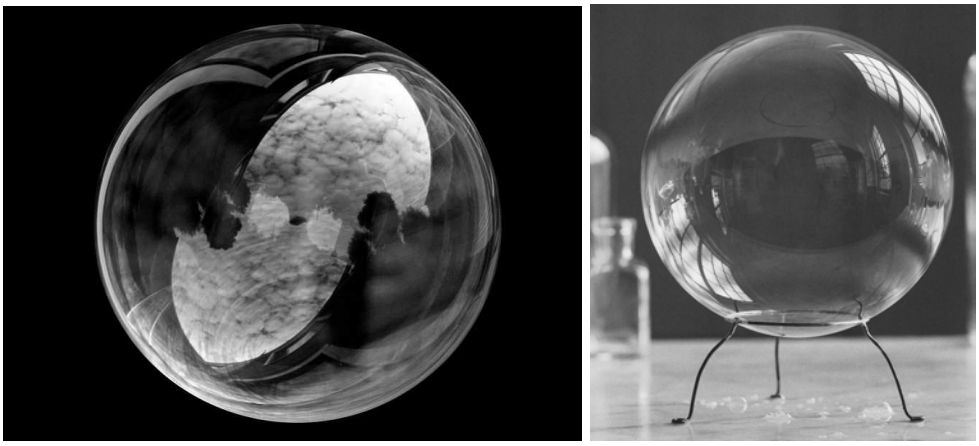

Figure 5.2. Left: Free-floating, nearly perfect spherical soap bubble with reflection of clouds (Mila Zinkova. Permission to be obtained). **Right:** Nearly spherical supported bubble. Permission to be obtained from [Wick 1997].

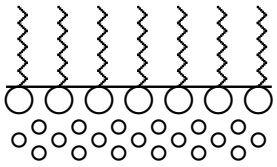

Schematic structure of a monolayer of soap molecules on a horizontal water surface. The hydrophobic tails stick out in the air with the hydrophilic heads buried in water (small circles).

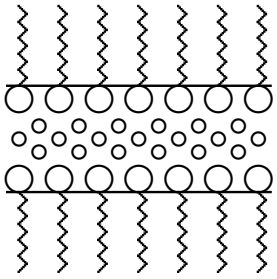

Schematic structure of a bilayer of soap molecules. The hydrophobic tails stick out on both sides of the membrane while the hydrophilic heads are buried in the thin layer of water.

A suitable *surfactant* [Gennes et al. 2002, ch. 7], for example soap, can stabilize the skin. Soap molecules are salts of fatty acids with hydrophilic (electrically charged) heads and hydrophobic (neutral) tails, making soap "love" both watery and fatty substances. This is the main reason why we use soap as detergent for washing; another is that the surface tension of soapy water is only about one third of that of pure water. Almost all surface impurities will in fact diminish surface tension of water because they reduce the fairly strong native attraction between water molecules. On the surface of soapy water, the soap molecules tend to orient themselves with their hydrophobic tails sticking out of the surface and their heads buried in the water. In a thin film of soapy water, the tails of the soap molecules stick out on both sides and form a bilayer with water in between.

The stabilizing effect of soap is primarily due to the coherence of the bilayer in conjunction with the lower surface tension of soapy water. When the soap film is stretched locally, the soap molecules are pulled apart and the surface tension increases because the intermolecular forces increase with distance (see figure 1.2 on page 5). Long before the structure of soap molecules was known, such a mechanism was suspected to lie behind bubble stability [Boys 1959]. Viscosity can also stabilize bubbles by slowing drainage, and this is why glycerin is often included in soap bubble recipes. The soap molecules crowding at the surface furthermore prolong the lifetime of a soap bubble by diminishing evaporation.

Mass of a bubble

A spherical air-filled soap bubble of radius R has two surfaces, one from air to soapy water and one from soapy water to air. Each gives rise to a pressure jump of $2\alpha/R$ where α is the monolayer surface tension. The total pressure inside a soap bubble is thus $\Delta p = 4\alpha/R$ larger than outside (although α is only about 1/3 of that of pure water). Taking $\alpha \approx 0.025$ N m^{-1} and a nominal radius $R \approx 10$ cm we find $\Delta p \approx 1$ Pa. The relative pressure increase is tiny, $\Delta p/p_0 \approx 10^{-5}$ where $p_0 \approx 1$ bar is the ambient air pressure. The ideal gas law (2.27) tells us that the relative density increase is the same, $\Delta\rho/\rho_0 = \Delta p/p_0$ where ρ_0 is the ambient air density. Whereas the true mass of the air in the nominal bubble is $M_0 = \frac{4}{3}\pi R^3\rho_0 \approx 5$ g, the effective mass of the air reduced by buoyancy is only $\Delta M = \frac{4}{3}\pi R^3\Delta\rho \approx 50\ \mu$g.

The play in spectral colors often seen in soap bubbles tells us that the thickness of the bubble skin may be comparable to the wavelength of light — about half a micrometer — which makes it about 1000 times thicker than the size of the hydrophilic head of a soap molecule. Taking the skin thickness of the nominal bubble to be constant, $\tau = 1\ \mu$m , the

mass of the water in the skin becomes $M_1 = 4\pi R^2 \tau \rho_1 \approx 0.13$ g where ρ_1 is the density of water. This is much larger than the effective mass of the air ΔM, and one may easily verify that the ratio $\Delta M/M_1 \approx 4 \times 10^{-4}$ is independent of the radius and thus the same for all soap bubbles with the nominal skin thickness.

Concluding, we have shown that buoyancy almost completely cancels the weight of the air in the bubble, so that the effective mass of the whole bubble always equals the mass of its skin, $M \approx M_1$ which comes to 0.13 gram for the nominal bubble. This tiny mass is the reason that even a gentle air current can make a bubble float away. In example 16.3 on page 277 we shall estimate the terminal fall velocity of fairly large spherical bubbles like this to be about 0.3 m/s, independent of the radius.

* The need for Marangoni forces

The weight of the bubble skin is the reason that surface tension cannot be perfectly constant in equilibrium but must increase when the skin is stretched. Suppose for definiteness that a bubble is falling with steady velocity through the air, only subject to the force of gravity and to drag-forces from the surrounding air. The external forces must of course cancel each other globally to secure steady motion, but will not cancel perfectly everywhere on the skin of the bubble. Whereas gravity acts in the same way all over the skin, drag acts most strongly on the lower part of the bubble, as does the wire frame support for the bubble at rest in figure 5.2 (right). Consequently, internal forces are necessary to secure that all parts of the bubble remain at rest with respect to each other.

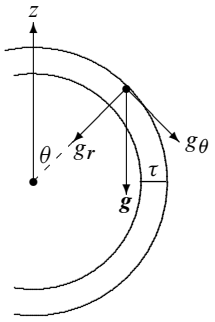

Gravity acting on the skin of the bubble, resolved in radial and tangential components, $g_r = -g_0 \cos\theta$ and $g_\theta = g_0 \sin\theta$.

Here we shall disregard drag and supporting forces and only discuss how internal forces locally can balance gravity on the upper part of the bubble. Consider a little circle on the sphere with fixed polar angle θ to the vertical. The mass of the skin in a small circular band $d\theta$ is $dM = \rho_1 \tau \cdot 2\pi R \sin\theta \cdot R d\theta$. The tangential component of its weight can only be balanced by a corresponding variation $d\alpha$ in surface tension of soapy water over the interval $d\theta$. Taking into account that the skin has two surfaces, the tangential force balance becomes $g_0 \sin\theta dM + 2\pi R \sin\theta \, 2d\alpha = 0$, or

$$\frac{d\alpha}{d\theta} = -\frac{1}{2}\rho_1 \tau R g_0 \sin\theta. \tag{5.6}$$

Assuming R to be nearly constant, the solution is $\alpha(\theta) = \alpha + \rho_1 \tau R g_0 \cos^2 \frac{1}{2}\theta$ where α is the surface tension of the unstretched surface at $\theta = 180°$. The weight of the lower half of the spherical bubble divided by the surface tension force acting on its rim is a dimensionless number, called the *Bond number*,

$$\mathsf{Bo} = \frac{2\pi R^2 \tau \rho_1 g_0}{2\pi R \alpha} = \frac{\tau R}{L_c^2} \tag{5.7}$$

where $L_c \approx 1.6$ mm is the capillary length of soapy water.

For the nominal bubble with $\tau = 1$ μm, $R = 10$ cm and $\alpha = 0.025$ N m^{-1} we find $\mathsf{Bo} = 0.04$. The relative variation in surface tension over the bubble is thus about 4% indicating that the skin must be stretched by a comparable amount to deliver the necessary elastic Marangoni forces. The radial component of the skin's weight also demands a local change in the bubble radius of the same magnitude to secure a constant pressure difference between the air inside and outside the bubble (see problem 5.7). For $R = 2.5$ m, the Bond number becomes unity, and the bubble undergoes major deformation, and perhaps breakup. You should probably never expect to encounter free-floating soap bubbles larger than a couple of meters[2].

[2]The largest free-floating bubble ever made had a volume of 2.98 m^3 corresponding to a spherical diameter of 1.79 meters [6].

5.3 Pressure discontinuity

The discontinuity in pressure across a spherical interface (5.4) is a special case of a general law discovered by Thomas Young (1805) and Pierre-Simon Laplace (1806). The law expresses the pressure discontinuity at a given point of an interface as the product of the local value of surface tension and twice the mean curvature of the interface. To derive this law and appreciate its power we need first to study some aspects of the local geometry of curves and surfaces.

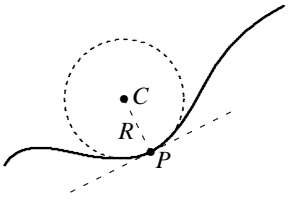

The local geometric properties of a smooth planar curve (fully drawn) near a given point are are approximated by the tangent (large dashes) and the osculating circle (small dashes) having the same tangent as the curve.

Local curvature of a planar curve

In the neighborhood of a given point P on a smooth planar curve, the behavior of the curve can be described geometrically by a series of increasingly precise approximations. In the first non-trivial approximation the curve is viewed as locally straight and approximated by its *tangent* in P. In the second approximation, the curve is viewed as locally circular and represented by its *osculating circle* in P with the same tangent as the curve. The radius R of the osculating circle is called the *radius of curvature* of the curve in the point P, and the center C which must necessarily lie on the normal to the tangent is called the *center of curvature*. The curve's *curvature* κ in P is defined as the inverse radius of curvature, $\kappa = 1/R$. As the point P moves along the smooth curve, both the direction of the tangent and the radius of curvature will change.

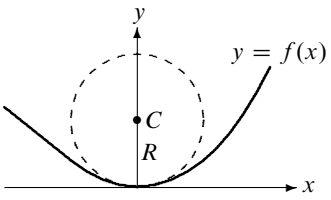

The curve $y = f(x)$ coincides near the origin with the osculating circle to second order in x.

To obtain a quantitative relation between the radius of curvature and the local properties of the curve, we introduce a local coordinate system with origin in the point P and the x-axis coinciding with the tangent in P. In this coordinate system the curve is described by a function $y = f(x)$ with $f(0) = f'(0) = 0$, so that to second order in x we have $y \approx \frac{1}{2}x^2 f''(0)$. In these coordinates the equation for the osculating circle is $x^2 + (y - R)^2 = R^2$ and for small x and y we find to leading order that $y \approx \frac{1}{2}x^2/R$. The osculating circle coincides with the curve $f(x)$ to second order when its curvature equals the second order derivative in P,

$$\frac{1}{R} = f''(0). \tag{5.8}$$

In problem 5.10 an expression is derived for the curvature at any point along a curve where the tangent is not necessarily parallel with the x-axis, but for now the above result suffices.

Notice that with this choice of coordinate system the radius of curvature is positive if the center of curvature lies above the curve, and negative if it lies below. The choice of sign is, however, pure convention, and there is no geometric significance associated with the sign of the radius of curvature in a particular point. What is significant are the changes of sign that may occur when comparing curvatures in different points.

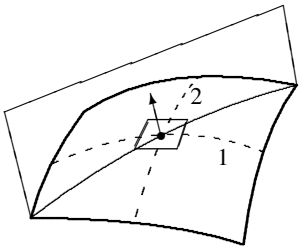

A plane containing the normal in a point of a surface intersects the surface in a planar curve. The extreme values of the signed radius of curvature defines the principal directions (dashed). The small rectangle has sides parallel with the principal directions.

Local curvature of a surface

Suppose you cut a smooth surface with a plane that contains the normal to a given point P on the surface. This plane intersects the surface in a smooth planar curve (a so-called normal section) with a radius of curvature R in the point P. The radius of curvature is given a conventional sign depending on which side of the surface the center of curvature is situated. As the intersection plane is rotated around the normal, the center of curvature moves up and down along the normal between the two extremes of the signed radius of curvature. The extreme radii, R_1 and R_2, are called the *principal radii of curvature* and the corresponding *principal directions* are orthogonal.

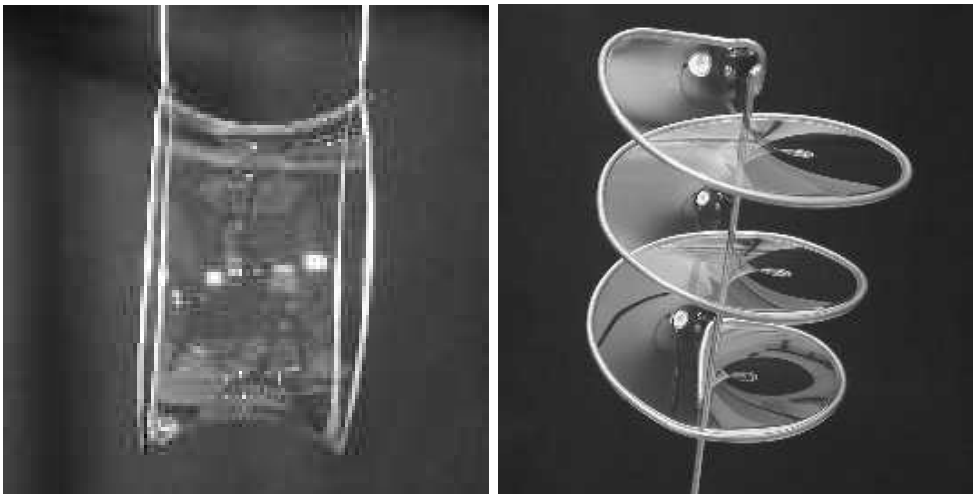

Figure 5.3. Soap films with zero mean curvature (Giorgio Carboni, permission to be obtained).

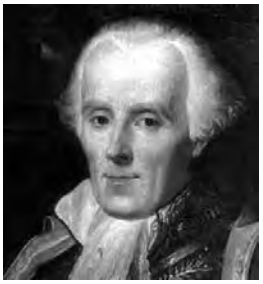

Pierre Simon marquis de Laplace (1749–1827). French mathematician, astronomer and physicist. Developed gravitational theory and applied it to perturbations in the planetary orbits and the conditions for stability of the solar system.

To prove these claims we introduce a local coordinate system with origin in P and the z-axis along the normal to the surface in P. To second order in x and y, the most general smooth surface is,

$$z = \frac{1}{2}ax^2 + \frac{1}{2}by^2 + cxy, \tag{5.9}$$

where a, b, and c are constants. Introducing polar coordinates $x = r\cos\phi$ and $y = r\sin\phi$, and using (5.8) we find the curvature of the normal section in the direction ϕ,

$$\frac{1}{R(\phi)} = \left.\frac{\partial^2 z}{\partial r^2}\right|_{r=0} = a\cos^2\phi + b\sin^2\phi + 2c\sin\phi\cos\phi. \tag{5.10}$$

Differentiating with respect to ϕ we find that the extremal values are determined by $\tan 2\phi = 2c/(a-b)$. Assuming $a \neq b$ this equation has two orthogonal solutions for $\phi = \phi_0 = \frac{1}{2}\arctan(2c/(a-b))$ and $\phi = \phi_0 + 90°$, and this proves our claim.

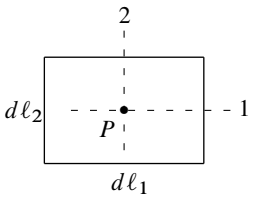

Tiny rectangle aligned with the principal directions, seen from "above". The sides are $d\ell_1$ and $d\ell_2$.

The Young-Laplace law

Consider now a small rectangle with sides $d\ell_1$ and $d\ell_2$ aligned with the principal directions in a given point of the surface, and let to begin with the principal radii of curvature, R_1 and R_2, be both positive. Surface tension pulls at this rectangle from all four sides, but the curvature of the surface makes each of these forces not quite parallel with the tangent plane. In the 1-direction surface tension acts with two nearly opposite forces of magnitude $\alpha d\ell_2$, each forming a tiny angle of magnitude $\frac{1}{2}d\ell_1/R_1$ with the tangent to the surface in the 1-direction. Projecting both of these forces on the normal we calculate the total force in the direction of the center of curvature C_1 as $d\mathcal{F} = 2\cdot\alpha d\ell_2\cdot\frac{1}{2}d\ell_1/R_1 = \alpha dA/R_1$ where $dA = d\ell_1\, d\ell_2$ is the area of the rectangle. Dividing by dA we obtain the excess in pressure $\Delta p = \alpha/R_1$ on the side of the surface containing the center of curvature. Finally, adding the contribution from the 2-direction we arrive at the *Young–Laplace* law for the pressure discontinuity due to surface tension,

$$\boxed{\Delta p = \alpha\left(\frac{1}{R_1} + \frac{1}{R_2}\right).} \tag{5.11}$$

For the sphere with $R_1 = R_2 = R$ we recover immediately the preceding result (5.4) .

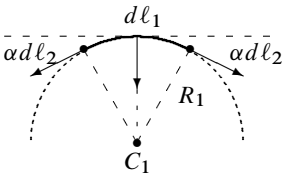

The rectangular piece of the surface with sides $d\ell_1$ and $d\ell_2$ is subject to two tension forces along the 1-direction resulting in a normal force pointing towards the center of curvature C_1. The tension forces in the 2-direction contribute analogously to the normal force.

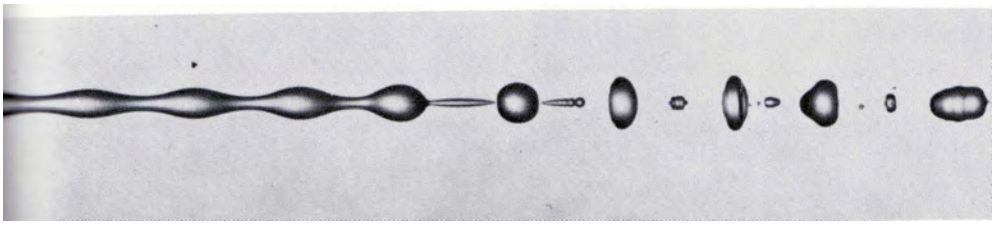

Figure 5.4. Breakup of a water jet emerging from a vertical tube (on the left) with diameter 4 mm. The picture has been turned 90° for graphical reasons. The jet is perturbed by the sound from a loudspeaker with a spatial wavelength corresponding to 4.6 diameters, which is somewhat larger than the Rayleigh–Plateau critical value of π diameters, but close to the wavelength of fastest breakup. Reproduced from [RJ71].

In using the Young–Laplace law it should be remembered that *each contribution to the pressure discontinuity is positive on the side of the surface containing the center of curvature, otherwise negative*. The Young-Laplace law is in fact valid if R_1 and R_2 are the radii of curvature of *any two orthogonal normal sections*, not necessarily along the principal directions, because it follows from eq. (5.10) that

$$\frac{1}{R(\phi)} + \frac{1}{R(\phi + 90°)} = a + b, \tag{5.12}$$

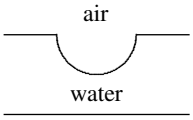

Sketch of the spherical meniscus formed by evaporation of water from the surface of a plant leaf. Surface tension creates a high negative pressure in the water, capable of lifting the sap to great heights.

which is independent of ϕ. The half sum of the reciprocal radii of curvature, $\frac{1}{2}(R_1^{-1} + R_2^{-1})$, is called the *mean curvature* of the surface in a given point. Soap films enclosing no air have the same pressure on both sides, $\Delta p = 0$, implying that the mean curvature must vanish everywhere. That does not mean that such films are planar. On the contrary, using suitable wireframes spectacular shapes can be created (see figure 5.3).

Example 5.1 [How sap rises in plants]: Plants evaporate water through tiny pores on the surface of their leaves. This creates a hollow air-to-water surface with radii of curvature comparable to the radius a of the pore. Both centers of curvature lie outside the water, leading to a *negative* pressure excess in the water. For a pore of one micron diameter, $2a \approx 1$ μm, the excess pressure inside the water will be about $\Delta p = -2\alpha/a \approx -3$ atm. This pressure is capable of lifting sap through a height of 30 m, but in practice, the lifting height is considerably smaller because of resistance in the xylem conduits of the plant through which the sap moves. Taller plants and trees need correspondingly smaller pore sizes to generate sufficient negative pressures, even down to -100 atm! Recent research has confirmed this astonishing picture [Tyr03, HZ08].

John William Strutt, 3rd Baron Rayleigh (1842–1919). Discovered and isolated the rare gas Argon for which he got the Nobel Prize (1904). Published the influential book 'The Theory of Sound' on vibrations in solids and fluids in 1877–78.

5.4 The Rayleigh–Plateau instability

The spontaneous breakup of the jet of water emerging from a thin pipe (see figure 5.4) is a well-known phenomenon, first studied by Savart in 1833. In spite of being blind, Plateau found experimentally in 1873 that the breakup begins when the water jet has become longer than its circumference. The observation was explained theoretically by Lord Rayleigh in 1879 as caused by the pressure discontinuity due to surface tension. Here we shall verify Plateau's conclusion in a simple calculation without carrying out a full stability analysis involving the dynamic equations of fluid mechanics (see the extensive review of liquid jets [EV08]).

Critical wavelength

Consider an infinitely long cylindrical column of incompressible liquid at rest in the absence of gravity with its axis along the z-axis. Due to the cylindrical form, surface tension will make

the pressure larger inside by $\Delta p = \alpha/a$ where a is its radius. This uniform pressure excess will attempt to squeeze the column uniformly towards a smaller radius, but if the column is infinitely long it will be impossible to move the liquid out of the way, and that allows us to ignore this problem.

What cannot be ignored, however, are local radial perturbations $r = r(z)$ that make the column bulge in some places and contract in others. The amount of extra liquid to move out of the way in response to pressure variations will then be finite. Any sufficiently small radial perturbation can always be resolved into a sum over perturbations of definite wave lengths (Fourier expansion), and to lowest order of approximation it is therefore sufficient to consider a harmonic perturbation with general wavelength λ and amplitude $b \ll a$ of the form,

$$r(z) = a + b\cos kz, \tag{5.13}$$

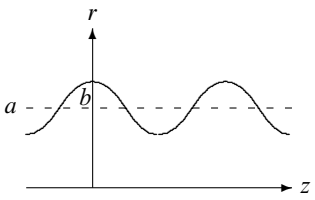

A harmonic perturbation $r(z) = a + b\cos kz$ of the radius of the fluid cylinder. The amplitude b of the perturbation is vastly exaggerated.

where $k = 2\pi/\lambda$ is the wave number. For tiny $b \ll a$ where the cylinder is barely perturbed, the two principal radii of curvature at any z become $R_1 \approx r(z) = a + b\cos kz$ and $1/R_2 \approx r''(z) = -bk^2\cos kz$, the latter obtained using (5.8) . To first order in b the pressure excess thus becomes,

$$\Delta p = \alpha\left(\frac{1}{R_1} - \frac{1}{R_2}\right) \approx \frac{\alpha}{a} + \frac{\alpha b}{a^2}\left(k^2a^2 - 1\right)\cos kz. \tag{5.14}$$

where we have chosen the explicit sign of R_2 such that both radii curvature contribute to the pressure excess in a bulge. The parenthesis in the last expression shows that there are now two radically different cases, depending on whether ka is larger or smaller than unity. Since $k = 2\pi/\lambda$, the so-called *critical value* of the wavelength corresponding to $ka = 1$ equals the circumference of the jet, $\lambda_c = 2\pi a$.

For $ka > 1$ or $\lambda < \lambda_c$, the pressure is higher in the bulges ($\cos kz > 0$) than in the constrictions ($\cos kz < 0$). Consequently, the liquid will be driven away from the bulges and into the constrictions, thereby diminishing the amplitude b of the perturbation and thus the pressure difference. The liquid seeks back towards the unperturbed state and the column is therefore *stable* in this regime.

Conversely, for $ka < 1$ or $\lambda > \lambda_c$, the pressure is higher in the constrictions than in the bulges, and liquid will be driven away from the constrictions and into the bulges, thereby increasing the amplitude of the perturbation. As seen in figure 5.4, the instability leads in the end to breakup of the column into individual drops, although this cannot be demonstrated by analyzing only infinitesimal perturbations as we have done here.

Joseph Antoine Ferdinand Plateau (1801–1883). Belgian experimental physicist. Created early cinematic effects from static images using his "Phenakistiscope". Studied soap bubbles extensively. In 1829 he stared into the Sun for 25 seconds to study the aftereffects in the eye, an experiment which he believed lead to his total loss of vision about 14 years later (although unrelated disease may have been the primary cause).

* Breakup time scale

Although we are not in position to make a full dynamic analysis along the lines of Rayleigh [Ray79], we shall set up an approximative dynamics that allows us to model the time evolution of the perturbed liquid column and make a decent estimate of the characteristic breakup time scale.

Before getting into the meat of a calculation, it is often useful to make a *dimensional analysis*. From the physics of the problem we surmise that the breakup time scale τ can only be a function of the radius a, the density ρ and the surface tension α, i.e. $\tau = f(a, \rho, \alpha)$. Since the dimension of density is kg m^{-3} and the dimension of surface tension is kg s^{-2}, the ratio ρ/α has dimension s^2 m^{-3}. To obtain a time we must multiply with the third power of the radius a, and then take the squareroot, to get the unique form,

$$\tau \sim \sqrt{\frac{a^3\rho}{\alpha}}. \tag{5.15}$$

The only thing that is missing is the constant in front which cannot be obtained by dimensional analysis, but requires a serious dynamical calculation.

Figure 5.5. The Rayleigh-Plateau instability makes it quite difficult to coat a fiber by pulling it out of a liquid bath, even if the liquid does wet a horizontal sheet of the fiber material. Spiders use this instability to deposit globules of glue with regular spacing on their snare lines. In the picture a film of silicone oil deposited on a cylindrical wire breaks up in a regular pattern of beads due to the instability. In this case the radius of the wire (0.1 mm) is so small that gravity has no influence. Reproduced from [LSQ06], permission to be obtained.

Our dynamical approximation consists in picking a half wavelength section of the liquid column between a minimum and maximum of the perturbation, and enclose it between solid walls (see the margin figure). The perturbed liquid column can be viewed as consisting of such sections. To first order in b, the volume of the liquid in half the bulge is

$$\int_0^{\lambda/4} \pi \left(r(z)^2 - a^2\right)\, dz \approx 2\pi ab \int_0^{\lambda/4} \cos kz\, dz = ab\lambda$$

Since the liquid is incompressible, the whole liquid column section must simultaneously be shifted along the axis through an distance z to build up the bulge. Equating the volume of shifted liquid with the volume in the bulge, $\pi a^2 z = ab\lambda$, we get $z = b\lambda/\pi a$.

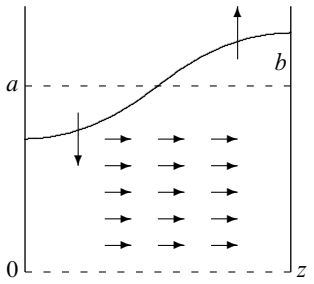

An increase in the amplitude b of the perturbation leads to a "horizontal" flow towards the right along the column axis.

The shift in the column section is driven by the pressure difference between minimum and maximum

$$\delta p = \Delta p|_{kz=\pi} - \Delta p|_{kz=0} = 2\frac{\alpha b}{a^2}\left(1 - k^2a^2\right). \tag{5.16}$$

Newton's second law for the column section becomes $Md^2z/dt^2 = \mathcal{F}_z$ where $M = \frac{1}{2}\pi a^2\lambda\rho$ is the mass of the column and $\mathcal{F}_z = \pi a^2\delta p$ is the driving force. Putting it all together we arrive at the following equation of motion for b,

$$\frac{d^2b}{dt^2} = \frac{b}{\tau^2} \qquad \text{with} \qquad \frac{1}{\tau^2} = \frac{\alpha}{\pi a\rho}k^2\left(1 - k^2a^2\right). \tag{5.17}$$

This confirms that in the unstable regime, $ka < 1$, the amplitude grows exponentially, $b = b_0 \exp(t/\tau)$, from an initial amplitude b_0. In the stable regime, $ka > 1$, it oscillates instead harmonically.

Normally the column is perturbed by a superposition of many wavelengths, but the one that corresponds to the smallest value of τ will completely dominate the sum at large times because of the exponential growth in the unstable regime. As a function of the wave number k, the right hand side of $1/\tau^2$ is maximal for $k^2a^2 = 1/2$, and this shows that the minimal breakup time scale and its corresponding wavelength are,

$$\tau_{\min} = \sqrt{\frac{4\pi a^3\rho}{\alpha}}, \qquad \lambda_{\min} = 2\pi\sqrt{2}\,a = \sqrt{2}\,\lambda_c\,. \tag{5.18}$$

At the fastest time scale the jet is chopped into pieces of size $\lambda_{\min}$ which is $\pi\sqrt{2} \approx 4.44$ times its diameter (Rayleigh [Ray78] obtained 4.508). This is why the jet in figure 5.4 is perturbed harmonically with a wavelength of 4.6 diameters. In figure 5.4 the jet diameter is 4 mm, implying $\lambda_{\min} = 18$ mm and $\tau_{\min} = 40$ ms. In problem 5.9 it is calculated that the broken liquid column turns into spherical drops with diameter nearly double the column diameter.

5.5 Contact angle

The two-dimensional interface between two homogeneous fluids makes contact with a solid container wall along a one-dimensional *contact line*. For the typical case of a three-phase contact between solid, liquid and gas the *contact angle* χ is defined as the angle between the solid and the interface (inside the liquid). Water and air against clean glass meet in a small acute contact angle, $\chi \approx 0°$, whereas mercury and air meets glass at an obtuse contact angle of $\chi \approx 140\,°$. Due to its small contact angle, water is very efficient in *wetting* many surfaces, whereas mercury has a tendency to contract into pearls.

It should be emphasized that the contact angle is extremely sensitive to surface properties, fluid composition, and additives. This is especially true for the water-air-glass contact angle. In the household we regularly use surfactants that diminish both surface tension and contact angle, thereby enabling dishwater better to wet greasy surfaces on which it otherwise would tend to pearl. Oppositely, after washing our cars we apply a wax which makes rainwater pearl and prevents it from wetting the surface, thereby diminishing rust and corrosion.

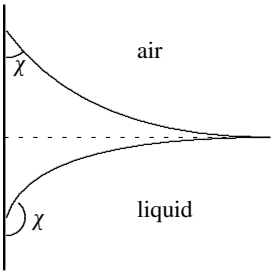

An air/liquid interface meeting a solid wall. The upper curve makes an acute contact angle, like water, whereas the lower curve makes an obtuse contact angle, like mercury.

Young's law

The contact angle is a material constant which depends on the properties of all three materials coming together. Whereas material adhesion can maintain a tension normal to the solid wall, the tangential tension has to vanish at the contact line, or it will start to move. This yields an equilibrium relation due to Thomas Young (1805)[3],

$$\alpha_{\mathrm{sg}} = \alpha_{\mathrm{sl}} + \alpha \cos\chi, \tag{5.19}$$

where α_{sg} and α_{sl} denote the solid/gas and solid/liquid surface tensions. Given the three surface tensions, we may directly calculate the contact angle,

$$\cos\chi = \frac{\alpha_{\mathrm{sg}} - \alpha_{\mathrm{sl}}}{\alpha} \tag{5.20}$$

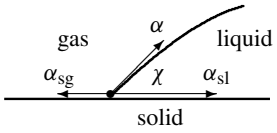

Liquid and gas meeting at a solid wall in a line orthogonal to the paper. The tangential component of surface tension along the wall must vanish.

This expression is, however, not particularly useful because the three surface tensions are not equally well known. As shown in the example below, estimates can sometimes be carried out which lead to reasonable values for the contact angle. It is, however, normally better to view χ as an independent material constant that can be directly measured.

The condition for existence of an equilibrium contact angle is evidently that the cosine lies between -1 and $+1$. For $0 < \alpha_{\mathrm{sg}} - \alpha_{\mathrm{sl}} < \alpha$ the contact angle is acute, $0 < \chi < 90°$, and the contact is said to be *mostly wetting*, while for $-\alpha < \alpha_{\mathrm{sg}} - \alpha_{\mathrm{sl}} < 0$ the contact angle is obtuse, $90° \leq \chi \leq 180°$, and the contact is said to be *mostly non-wetting* [Gennes et al. 2002]. If on the other hand $\alpha_{\mathrm{sg}} - \alpha_{\mathrm{sl}} > \alpha$, the contact line cannot be static, but will be drawn towards the gas while dragging the liquid along, and thereby spreading it all over a horizontal surface. Such a contact is said to be *completely wetting*. Similarly, if $\alpha_{\mathrm{sg}} - \alpha_{\mathrm{sl}} < -\alpha$, the contact is *completely non-wetting* and the contact line will recede from the gas on a horizontal surface until all the liquid collects into nearly spherical pearls (a phenomenon called *dewetting*).

A large amount of recent research concerns the dynamics of contact lines under various conditions (see [Gennes et al. 2002] and [Gen85]). In the following we shall limit the analysis to static contact lines with a well-defined contact angle.

[3]Sometimes this law is called the Young-Dupré law, thereby crediting the French mathematician/physicist Athanase Dupré (1808–1869) for relating this law to the thermodynamic work function for adhesion.

Example 5.2 [Contact angle of water on ice]: An estimate of the contact angle of water on ice at 0°C can be obtained from the latent heats of evaporation of liquid water, and from the latent heats of melting and sublimation of ice. For liquid water the molar enthalpy of evaporation is $h_{\rm evap} = 45.051$ kJ/mol, whereas for ice the molar enthalpy of melting is $h_{\rm melt} = 6.010$ kJ/mol and the molar enthalpy of sublimation $h_{\rm subl} = 51.059$ kJ/mol [7]. Notice that $h_{\rm subl} = h_{\rm melt} + h_{\rm evap}$ as one would expect. Using the densities $\rho_{\rm ice} = 916.72$ kg m^{-3} and $\rho_{\rm water} = 1000$ kg m^{-3} at 0°C, we find from eq. (5.1) the following values $\alpha_{\rm sg} = 0.138$ N m^{-1}, $\alpha_{\rm sl} = 0.016$ N m^{-1}, and $\alpha = 0.129$ N m^{-1}. From eq. (5.20) we estimate $\cos\chi \approx 0.95$ or $\chi \approx 19°$ which is quite reasonable because the value is quoted to lie between 12° and 24° [VSM02].

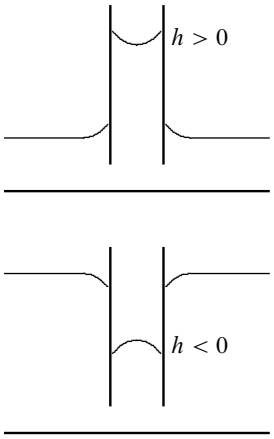

Top: Water rises above the ambient level in a glass tube and displays a concave meniscus inside the tube. **Bottom:** Mercury sinks below the general level in a capillary glass tube and displays a convex meniscus.

James Jurin (1684–1750). English physician. An ardent proponent of Newton's theories. Credited for the discovery of the inverse dependence of the capillary height on the radius of the tube in 1718, although others had noticed it before [Gennes et al. 2002, p. 49].

Capillary effect

Water has a well-known ability to rise above the ambient level in a narrow, vertical, cylindrical glass tube that is lowered into the liquid. This is called the *capillary effect* and takes place because the surface tension of glass in contact with air is larger than that of glass in contact with water, $\alpha_{\rm sg} > \alpha_{\rm sl}$. The water rises to height h where the upwards force due to the difference in surface tension balances the downwards weight of the raised water column (disregarding the volume of the meniscus-shaped surface),

$$(\alpha_{\rm sg} - \alpha_{\rm sl})2\pi a \approx \rho_0 g_0 \pi a^2 h. \tag{5.21}$$

Using the Young law (5.19) we arrive at *Jurin's height*

$$\boxed{h \approx 2\frac{L_c^2}{a}\cos\chi.} \tag{5.22}$$

where L_c is the capillary length (5.5) . The height is positive for acute contact angles ($\chi < 90°$) and negative for obtuse ($\chi > 90°$). It fairly obvious that the approximation of ignoring the shape of the meniscus is equivalent to assuming that the tube radius is much smaller than the capillary length, $a \ll L_c$. In section 5.7 we shall determine the exact shape of the surface meniscus for any tube radius.

For mostly wetting liquids, the rise may also be seen as caused by the acute contact angle at the water-air-glass contact line which makes the surface inside the tube concave, such that the center of curvature lies outside the liquid. Surface tension will create a negative pressure just below the liquid surface, and that is what lifts the water column (as in example 5.1). Mercury with its obtuse contact angle displays instead a convex surface shape, creating a positive pressure jump which makes the liquid drop down to a level where the pressure just below the surface equals the ambient hydrostatic pressure at the same level outside.

When the tube radius a is small compared to the capillary length L_c, gravity has no effect on the shape, and the surface may be assumed to be part of a sphere of radius R. The geometric construction in the margin figure yields the tube radius $a \approx R\cos\chi$ and the central depth $d \approx R(1 - \sin\chi)$. Eliminating R we obtain,

$$\boxed{d \approx a\frac{1-\sin\chi}{\cos\chi}.} \tag{5.23}$$

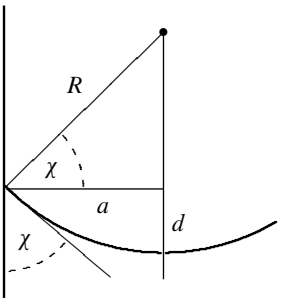

Approximately spherical surface with acute contact angle in a narrow circular tube.

Both the capillary depth and the capillary height are as mentioned modified for larger radius, $a \gtrsim L_c$, where the surface flattens in the middle.

Example 5.3: A certain capillary tube has diameter $2a = 1$ mm. Water with $\chi \approx 0°$ and $L_c \approx 2.7$ mm rises to $h = +30$ mm with a surface depth $d = +0.5$ mm. Mercury with contact angle $\chi \approx 140°$ and $L_c = 1.9$ mm sinks on the other hand to $h = -11$ mm and depth $d = -0.2$ mm under the same conditions.

Figure 5.6. Spider walking on water. This is also an effect of surface tension. Image courtesy David L. Hu, MIT (see also [HCB03] for analysis of the physics of water striding).

Case: Walking on water

Many species of animals—mostly insects and spiders— are capable of walking on the surface of water (see figure 5.6 and the comprehensive review [BH06b]). Compared to the displacement necessary to float, only a very small part of the water-walking animal's body is below the ambient water surface level. The animal's weight is mostly carried by surface tension while buoyancy — otherwise so important for floating objects — is negligible.

The water is deformed by the animal's weight and makes contact with its "feet" along a total (combined) perimeter length L. The animal must somehow "wax its feet" to obtain an obtuse contact angle $\chi > 90°$ so they avoid getting wet. In a given contact point, the angle between the tangent to the "foot" and the undeformed water surface is denoted θ (see the margin figure). For simplicity we shall assume that this angle is the same everywhere along the perimeter curve. Surface tension acts along the tangent to the deformed water surface and simple geometry tells us that the angle of this force with the vertical is $\psi = 90° - \theta + 180° - \chi$. Projecting the surface tension on the vertical, we obtain the following condition for balancing the animal's weight,

$$\alpha L \cos\psi = M g_0. \tag{5.24}$$

The ratio between the weight and surface tension force is called the *Bond number*,

$$\boxed{\mathsf{Bo} = \frac{M g_0}{\alpha L},} \tag{5.25}$$

where M is the mass of the animal. If $\mathsf{Bo} < 1$ surface tension is capable of carrying the weight of the animal with and angle determined by $\cos\psi = \mathsf{Bo}$. If $\mathsf{Bo} > 1$ this is not possible, and the animal literally falls through. The reciprocal number $\mathsf{Je} = 1/\mathsf{Bo}$ which must be larger than unity for anyone who wants to walk on water has — with tongue in cheek — been called the *Jesus number* [Vogel 1988].

An insect with mass $M = 10$ mg requires the total length L of the contact perimeter to be larger than 1.3 mm to make $\mathsf{Bo} < 1$. Heavier animals need correspondingly larger feet.

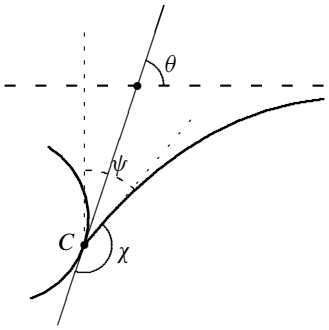

Geometry of water-walking with a contact line through C. The arc on the left represents the "foot", and the curve on the right the deformed water surface. The contact angle is χ and the angle between the tangent and the horizontal undeformed water surface (dashed) is θ. Surface tension acts along the tangent (dotted) to the deformed water surface. Its projections on the vertical (dashed) through the angle ψ must add up to the animal's weight.

5.6 Meniscus at a flat wall

Even if the capillary effect is best known from cylindrical tubes, any fluid interface will take a non-planar shape near a solid wall where the interface rises or falls relative to the ambient horizontal fluid level. The crescent shape of the interface is called a *meniscus*. A vertical flat wall is the simplest possible geometry, and in this case there is no capillary effect because the interface must approach the ambient level far from the wall. Taking the x-axis horizontal and the z-axis vertical, the meniscus shape may be assumed to be independent of y and described by a simple planar curve $z = z(x)$ in the xz-plane.

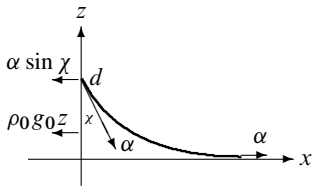

The meniscus starts at the wall with the given contact angle (here acute) and approaches the ambient interface level far from the wall.

The height at the wall

The meniscus height d at the wall can be calculated exactly by balancing the external horizontal forces acting on the fluid (see the margin figure). Far from the wall for $x \to \infty$ the force (per unit of y) is just α whereas at the wall for $x = 0$ there is the wall's reaction $\alpha \sin\chi$ to the pull from the surface itself plus its reaction to the hydrostatic pressure exerted by the fluid, $\int_0^d \rho_0 g_0 z\, dz = \frac{1}{2}\rho_0 g_0 d^2$. The equation of balance thus becomes

$$\alpha \sin\chi + \frac{1}{2}\rho_0 g_0 d^2 = \alpha,$$

which yields

$$d = L_c\sqrt{2(1-\sin\chi)} = 2L_c \sin\frac{90^\circ - \chi}{2}. \tag{5.26}$$

Although derived for acute contact angles, the last expression is also valid for obtuse angles. It should be emphasized that this is an exact result. For water with $\chi \approx 0$ we find $d \approx \sqrt{2}L_c \approx 3.9$ mm, whereas for mercury with $\chi = 140^\circ$ we get $d \approx -1.6$ mm.

Geometry of planar curves

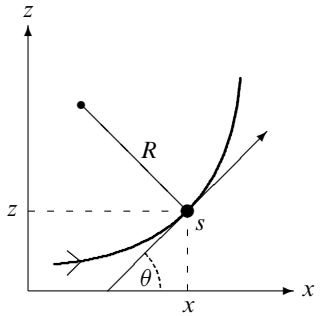

The geometry of a planar oriented curve. The curve is parameterized by the arc length s along the curve. A small change in s generates a change in the elevation angle θ determined by the local radius of curvature. Here the radius of curvature is positive.

The best way to handle the geometry of a planar oriented curve is to introduce two auxiliary parameters: the *arc length* s along the curve, and the *elevation angle* θ between the x-axis and the oriented tangent to the curve. Due to the monotonic increase of arc length as a point moves along the oriented curve, it is mostly convenient to parameterize the curve by means of the arc length, $\theta = \theta(s)$, $x = x(s)$, and $z = z(s)$.

A small increment $s \to s + ds$ in the arc length moves the point (x, z) an amount (dx, dz) along the tangent, and we obtain immediately from the definition of θ, and the fact that $ds = R\, d\theta$,

$$\frac{dx}{ds} = \cos\theta, \qquad \frac{dz}{ds} = \sin\theta, \qquad \frac{d\theta}{ds} = \frac{1}{R}\,. \tag{5.27}$$

If the elevation angle θ is an increasing function of the arc length s, the radius of curvature R must be taken to be positive, otherwise negative. One should be aware that this sign convention may not agree with the physical sign convention for the Young–Laplace law (5.11) . Depending on the arrangement of the fluids with respect to the interface, it may — as we shall now see — be necessary to introduce an explicit sign to get the physics right.

The meniscus equation

To obtain an expression for the geometric radius of curvature we employ hydrostatic balance at every point of the meniscus. For simplicity we assume that there is air above the liquid and that the air pressure on the interface is constant, $p = p_0$. Then the pressure in the liquid just below the surface is $p = p_0 + \Delta p$ where Δp is given by the Young–Laplace law (5.11) . In terms of the local geometric radius of curvature R, we have for an acute angle of contact $R_1 = -R$ because the center of curvature of the concave meniscus lies outside the liquid. The other principal radius of curvature is infinite, $R_2 = \infty$, because the meniscus is flat in the y-direction.

The pressure just below the surface, $p = p_0 - \alpha/R$, is always smaller than atmospheric. Since surface tension does not change the equation of hydrostatic equilibrium, the pressure in the liquid will — as in the sea (page 22) — be constant at any horizontal level z, and given by $p = p_0 - \rho_0 g_0 z$ where p_0 is the ambient pressure. Just below the surface $z = z(s)$ we have,

$$p_0 - \rho_0 g_0 z = p_0 - \frac{\alpha}{R}, \tag{5.28}$$

and using this equation to eliminate $1/R$ we obtain from (5.27)

$$\frac{d\theta}{ds} = \frac{z}{L_c^2}, \tag{5.29}$$

where we have also introduced the capillary length L_c defined in eq. (5.5) . Differentiating the above equation once more with respect to s and making use of (5.27) , we obtain

$$\boxed{L_c^2 \frac{d^2\theta}{ds^2} = \sin\theta.} \tag{5.30}$$

This second order ordinary differential equation for the planar meniscus is expressed entirely in the elevation angle $\theta = \theta(s)$.

Pendulum connection: The meniscus equation (5.30) is nothing but the equation for an *inverted mathematical pendulum*. A mathematical pendulum of length ℓ and unit mass obeys Newton's second law in a constant field of gravity g (see the margin figure),

$$\ell \frac{d^2\phi}{dt^2} = -g \sin\phi.$$

Taking $\phi = 180^\circ - \theta$ and $t = \sqrt{\ell/g} = s/L_c$ we arrive at the meniscus equation. Although it is amusing to translate the solutions to the meniscus equation into pendulum motions, we shall not exploit this connection further here.

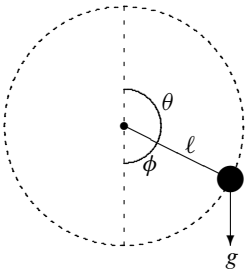

A mathematical pendulum. The angle ϕ is measured from stable equilibrium $\phi = 0$. The elevation angle is $\theta = 180^\circ - \phi$.

Analytic solution

Since L_c is the only length scale in the problem we may without loss of generality take $L_c = 1$, so that all lengths are measured in units of L_c. Multiplying the meniscus equation (5.30) with $d\theta/ds$, its first integral becomes

$$\frac{1}{2}\left(\frac{d\theta}{ds}\right)^2 = 1 - \cos\theta. \tag{5.31}$$

The constant on the right hand side has been determined from the conditions that $\theta \to 0$ and $d\theta/ds \to 0$ for $s \to \infty$. From this equation we get

$$\frac{d\theta}{ds} = \sqrt{2(1-\cos\theta)} = -2\sin\frac{\theta}{2} \tag{5.32}$$

where we have used that the contact angle is acute so that $d\theta/ds > 0$ and $\theta < 0$ (see the margin figure).

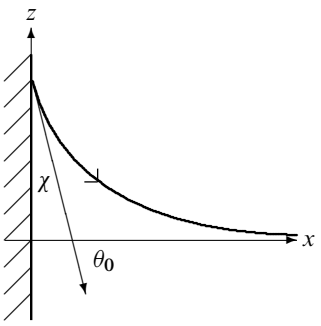

Geometry of single plate meniscus for acute contact angle $\chi < 90^\circ$. The elevation angle θ is always negative with initial value $\theta_0 = \chi - 90^\circ$ at the wall for $s = 0$. The other initial values are $x = 0$, $z = d$ for $s = 0$.

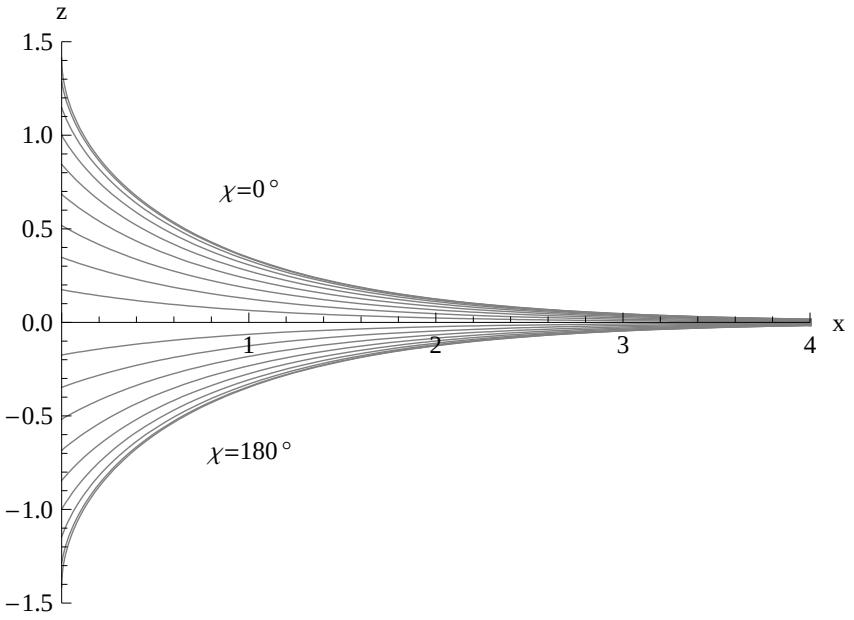

Figure 5.7. Flat-wall meniscus (in units of $L_c = 1$) for all contact angles in steps of 10°. Close to the wall the menisci are linear and far from the wall they approach the x-axis exponentially.

Combining this equation and (5.27) we obtain, using well-known trigonometric relations,

$$\frac{dx}{d\theta} = \sin\frac{\theta}{2} - \frac{1}{2\sin\frac{\theta}{2}}\,, \qquad \frac{dz}{d\theta} = -\cos\frac{\theta}{2}\,. \tag{5.33}$$

Finally integrating these equations we get the meniscus shape in parametric form,

$$\boxed{x = 2\cos\frac{\theta_0}{2} + \log\left|\tan\frac{\theta_0}{4}\right| - 2\cos\frac{\theta}{2} - \log\left|\tan\frac{\theta}{4}\right|, \qquad z = -2\sin\frac{\theta}{2}\,.} \tag{5.34}$$

The integration constant is chosen such that $x = 0$ for $\theta = \theta_0 = \chi - 90°$ and $z \to 0$ for $\theta \to 0$. The solution is valid for both acute and obtuse contact angles, and is plotted in figure 5.7 for a selection of contact angles.

At the wall the meniscus height becomes

$$d = z(\theta_0) = 2\sin\frac{90° - \chi}{2}\,, \tag{5.35}$$

which is identical to the earlier result (5.26) . Far from the wall for $\theta \to 0$, we have $x \approx -\log|\theta/4|$ and $z \approx -\theta$, so that

$$z \approx \pm 4e^{-x}. \tag{5.36}$$

The meniscus decays exponentially with a sign depending on whether the contact angle is acute or obtuse.

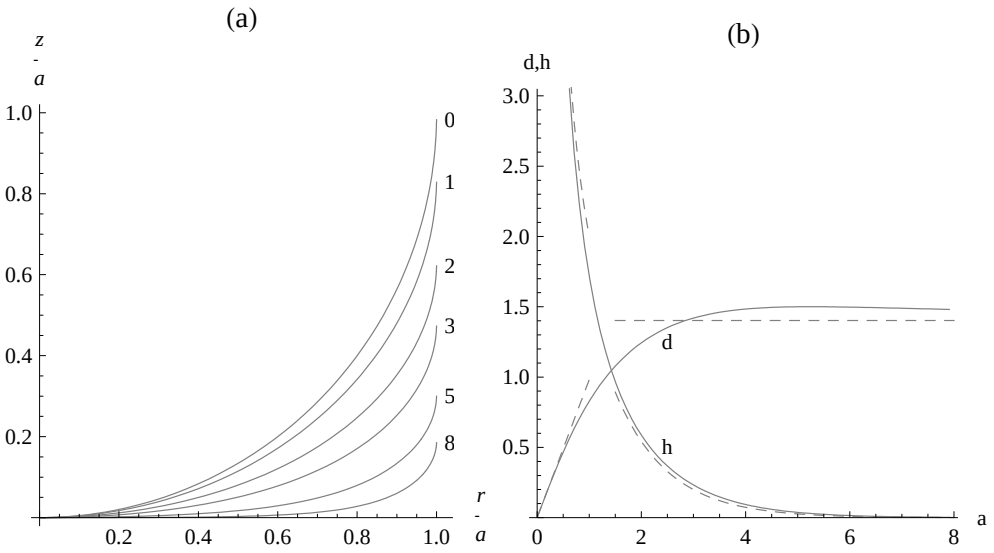

Figure 5.8. Meniscus and capillary effect in "water" with $\chi = 1°$ for a cylindrical tube of radius a in units where $L_c = 1$. **(a)** Meniscus shape $z(r)/a$ plotted as a function of r/a for $a \to 0$ and $a = 1, 2, 3, 5, 8$. Note how the shape is nearly spherical for $a \lesssim 1$ and essentially independent of a. **(b)** Computed capillary height h and depth d as functions of a (solid lines). The dashed curves are the meniscus estimates (5.42) .

5.7 Meniscus in cylindrical tube

Many static interfaces, for example the meniscus in a cylindrical tube but also droplets and bubbles are invariant under rotation around an axis, allowing us to establish a fairly simple formalism for the shape of the interface, similar to the two-dimensional formalism of the preceding section.

Geometry of axial surfaces

In cylindrical coordinates an axially invariant surface is described by a planar curve in the rz-plane. Using again the arc length s along the curve and the angle of elevation θ for its slope, we find as in the planar case,

$$\frac{dr}{ds} = \cos\theta, \qquad \frac{dz}{ds} = \sin\theta. \tag{5.37}$$

The first principal radius of curvature may be directly taken from the two-dimensional case, whereas it takes some work to show that the second center of curvature lies on the z-axis (see problem 5.3), such that the radial distance becomes $r = R_2 \sin\theta$, so that

$$\frac{d\theta}{ds} = \frac{1}{R_1}, \qquad \frac{\sin\theta}{r} = \frac{1}{R_2}. \tag{5.38}$$

Since R_2 is known as a function of θ and r, we just need an expression for $R_1 = R_1(r, z, \theta, s)$ to close this set of equations.

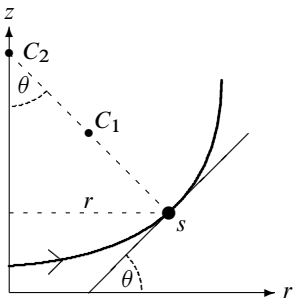

The oriented curve is parameterized by the arc length s. A small change in s generates a change in the elevation angle θ determined by the local radius of curvature R_1 with center C_1. The second radius of curvature R_2 lies on the z-axis with center C_2 (see problem 5.3).

Alternatively one may use the Young-Laplace expression (5.11) for the mean curvature,

$$\frac{d\theta}{ds} + \frac{\sin\theta}{r} = \frac{1}{R_1} + \frac{1}{R_2} = \frac{\Delta p}{\alpha}. \tag{5.39}$$

As before, one should keep in mind that the sign convention for the geometric radii of curvature may not agree with the physical sign convention for the Young–Laplace law (5.11) , and that one must be careful to get the sign of Δp right.

A special class of solutions is given by the open soap film surfaces with vanishing mean curvature, $\Delta p = 0$, as seen in figure 5.3. Their shapes are entirely dependent on the boundary conditions provided by the the stiff wire frames used to create and maintain them. There is essentially only one axially symmetric shape namely the one in figure 5.3a (see problem 5.13).

Numeric solution

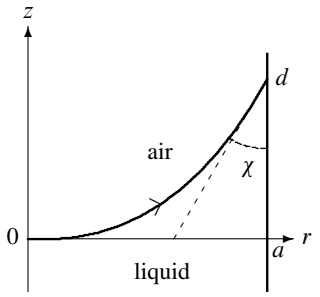

Meniscus with acute angle of contact. Both centers of curvature lie outside the liquid.

For the liquid/air meniscus with acute contact angle the geometric radii of curvature are positive, and since both centers of curvature lie outside the liquid, the pressure will be larger outside than inside. For convenience we choose the ambient liquid level to be $z = -h$ where h is the (so far unknown) capillary height in the center of the tube. The pressure in the liquid is $p = p_0 - \rho_0 g_0(z + h)$ where p_0 is the atmospheric pressure. The pressure jump from liquid to atmosphere therefore becomes

$$\Delta p = p_0 - p = \rho_0 g_0(z + h) \tag{5.40}$$

We have now obtained a closed set of three first-order differential equations for r, z and θ as functions of the arc length s.

Unfortunately these equations cannot be solved analytically, but given a value for the radius a and the contact angle χ they may be solved numerically as a boundary value problem in the interval $0 \le s \le s_0$ with the boundary conditions

$$r = 0, \qquad z = 0, \qquad \theta = 0, \qquad (s \to 0) \tag{5.41a}$$
$$r = a, \qquad z = d, \qquad \theta = 90^\circ - \chi, \qquad (s \to s_0) \tag{5.41b}$$

where d, h, and s_0 are unknown. Integrating, one obtains not only the functions $r(s)$, $z(s)$ and $\theta(s)$, but also the values of the unknown parameters h, d and s_0. The numeric solutions for the menisci in water with $\chi \approx 0$ are displayed in figure 5.7a for a selection of values of the radius a.

The corresponding capillary height h and depth d are shown as functions of a in figure 5.7b, and are compared with the small and large a approximations already obtained in (5.22) , (5.23) , (5.36) and (5.26) ,

$$h \approx 2\frac{L_c^2}{a}\cos\chi, \qquad d \approx a\frac{1-\sin\chi}{\cos\chi}, \qquad \text{for } a \ll 1. \tag{5.42a}$$
$$h \approx \pm 4L_c e^{-a/L_c}, \qquad d \approx 2L_c \sin\frac{90^\circ - \chi}{2}, \qquad \text{for } a \gg 1. \tag{5.42b}$$

In (5.36) have replaced z by h and x by a to get an estimate of the central height h. As seen from figure 5.7b, these approximations fit the numeric solutions quite well in their respective regions.

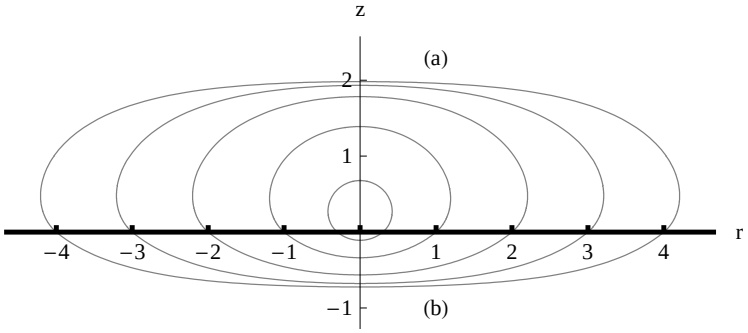

Figure 5.9. Shapes of sessile liquid droplets in air **(a)** , and captive air bubbles in the same liquid **(b)** . The contact angle is obtuse in both cases, $\chi = 140°$ (mercury). For the complementary contact angle $\chi = 40°$, the picture is simply turned upside down with the flat shapes on the top and the rounded ones on the bottom. All lengths in the figure are measured in units of the capillary length L_c.

* 5.8 Sessile drops and captive bubbles

Everyone is familiar with drops of liquid sitting stably (*i.e. sessile*) on top of a horizontal surface. Small droplets tend to be spherical in shape, but gravity flattens larger drops into puddles when their size exceeds the capillary length. On a wetting surface where the contact angle is tiny, water droplets are always quite flat and tend to spread out into thin layers. Mercury on the other hand with its obtuse contact angle of 140° against many solid surfaces is seen to form small, nearly spherical droplets. Larger mercury drops tend to form puddles that likewise can be hard to keep in place. The 'quickness' of mercury (also known as quicksilver) is mainly due its high density which makes gravity easily overcome surface adhesion, if for example the horizontal surface is tilted a tiny bit.

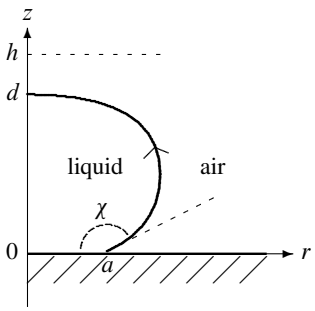

Geometry of sessile drop on a horizontal plate. The contact angle χ is here obtuse (as for mercury), the circular contact area (the droplet's 'footprint') has radius a, and the central height of the droplet is d.

Sessile drops

The coordinate system is chosen so that the plate surface is given by $z = 0$ (see the margin figure). Both centers of curvature lie inside the liquid so that the pressure is everywhere higher in the liquid than in the atmosphere. The pressure in the liquid is hydrostatic $p = p_1 - \rho_0 g_0 z$ where p_1 is the pressure at $z = 0$. Since the geometric radii of curvature are positive with the indicated orientation of the curve, the pressure jump is in this case the difference between liquid and atmospheric pressure,

$$\Delta p = p - p_0 = p_1 - p_0 - \rho_0 g_0 z = \rho_0 g_0 (h - z). \tag{5.43}$$

Here we have defined the height h by setting $p_1 - p_0 = \rho_0 g_0 h$. Since the radii of curvature are always positive, we must have $h > d$ such that the even the pressure on the top of the droplet at $z = d$ is always higher than atmospheric.

The solution of the three coupled first-order differential equations (5.37) and (5.39) now proceeds as in the preceding section. The boundary conditions are in this case

$$r = a, \qquad z = 0, \qquad \theta = 180° - \chi \qquad (s = 0), \tag{5.44a}$$

$$r = 0, \qquad z = d, \qquad \theta = 180° \qquad (s = s_0). \tag{5.44b}$$

Given the 'footprint' radius a and the contact angle χ, the droplet shapes and the unknown parameters d, h, and s_0 can be determined. The droplet shapes are shown in figure 5.9a for a choice of footprint radii and an obtuse contact radius $\chi = 140°$, corresponding to mercury on glass.

For $a \ll L_c$ the droplet is spherical while for $a \gg L_c$ it becomes a flat puddle (see figure5.9a). Estimating in the same way as before (see problem 5.5) we find

$$d \approx a\frac{1-\cos\chi}{\sin\chi} \quad \text{for } a \ll L_c, \qquad d \approx 2L_c \sin\frac{\chi}{2} \quad \text{for } a \gg L_c. \tag{5.45}$$

Mercury with $\chi = 140°$ has maximal puddle height $d \approx 1.88L_c$ in close agreement with figure 5.9a. Water on a wetting surface with $\chi \approx 1°$, has maximal puddle height $d \approx L_c\chi \approx 50\ \mu$m. A bucket of water thrown on the floor really makes a mess.

Captive bubbles

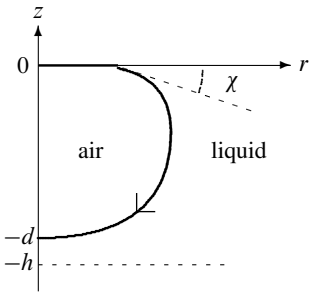

Captive air bubble under a horizontal lid in a liquid with acute angle of contact, for example in water.

Air bubbles may similarly be captured on the underside of a horizontal lid covering a liquid. In this case it is the buoyancy forces that press the bubble against the lid. If the bubble footprint is not too much smaller than the capillary length, there is only little compression of the air from surface tension, although there may be some overall compression due to the ambient hydrostatic pressure in the liquid at the bubble's level. Since the density of the air is normally much smaller than the density of the liquid, we may take the air pressure to be effectively constant, p_1, in the bubble. With the orientation of the margin figure both geometric radii of curvature are negative, implying that in this case Δp should be the pressure difference between liquid and gas which is also negative. The pressure in the liquid is $p = p_0 - \rho_0 g_0 z$, where p_0 is the pressure just under the lid, so that the pressure discontinuity between liquid and gas becomes

$$\Delta p = p - p_1 = p_0 - p_1 - \rho_0 g_0 z = -\rho_0 g_0 (z + h), \tag{5.46}$$

In the last expression we have introduced an artificial "height" h through $p_1 - p_0 = \rho_0 g_0 h$. This defines the level $z = -h$ where the pressure jump would vanish. Since the pressure discontinuity between liquid and gas is always negative, we must have $h > d$ where d is the height of the bubble.

The transformations $(r, z, \theta) \to (r, -z, -\theta)$ and $\Delta p \to -\Delta p$ leave eqs. (5.37) and (5.39) invariant. The bubble shapes may for this reason be obtained from the drop shapes provided one replaces the contact angle by its complement, $\chi \to 180° - \chi$. The bubble shapes are also shown in figure 5.9 below the horizontal line.

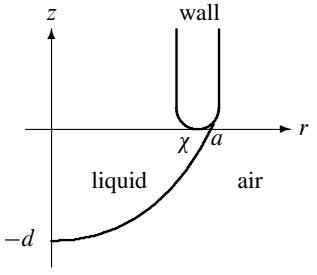

A liquid drop hanging from a tube with strongly exaggerated wall thickness. Any true contact angle can be accommodated by the 180° turn at the end of the tube's material. The apparent contact angle χ between the liquid surface and the horizontal can in principle take any value.

* 5.9 Pendant drops and tethered bubbles

Whereas sessile drops in principle can have unlimited size, pendant (hanging) liquid drops will detach and fall if they become too large. Likewise, air bubbles tethered to a solid object in a liquid will detach and rise if they grow too large. Here we shall only discuss pendant drops because the shapes of tethered bubbles are complementary to the shapes of pendant drops (like captive bubbles are complementary to sessile; see the preceding section). Drops can hang from all kinds of objects. Under a flat, horizontal plate drops may, for example, form from condensation. In that case the constraint is that the liquid has to have the correct contact angle with the plate.

A drop may also hang from the tip of a vertical capillary tube, for example a pipette fitted with a rubber bulb, through which liquid can be slowly injected to feed it. If the feeding rate is slow enough, the drop will grow through a sequence of equilibrium shapes with continuously increasing volume until it becomes unstable and detaches. The advantage of this arrangement is that the rounded end of the tube can accommodate any contact angle (see the margin figure). The constraint is in this case that all drop shapes must have the same footprint radius. We shall for simplicity also assume that the tube wall has vanishing thickness and that the three-phase contact line is fixed at the tip of the tube. The actual dynamics of the detachment of the drop

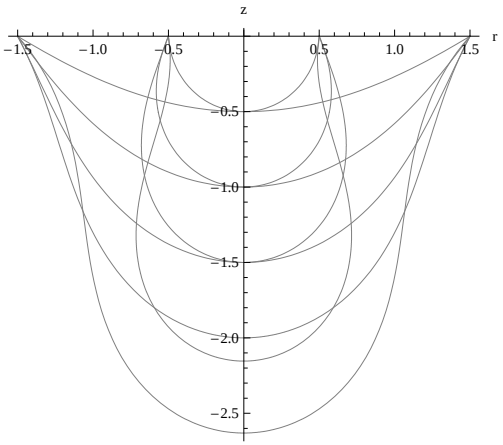

Figure 5.10. Two sets of static drop shapes hanging from the mouth of capillary tube with radius $a = 0.5$ and $a = 1.5$, respectively (in units where $L_c = 1$). For each set there is no static solution with larger volume than shown here, which indicates the limit to the size of the static shapes that can be created by slowly feeding the drops through the tubes.

is highly interesting, but cannot be studied within the hydrostatic framework of this chapter (see however [Egg97, WPB99]).

Tate's Law

The naive reason that a pendant droplet can be in stable equilibrium is that surface tension α pulls so strongly upwards at the rim of the tube that it overcomes the weight of the drop. Denoting the capillary tube radius by a and the angle between the liquid surface and the horizontal by χ, this condition becomes

$$Mg_0 < 2\pi a\alpha \sin\chi, \tag{5.47}$$

where M is the total mass of the drop. For the capillary, the right hand side is maximal for $\chi = 90°$, so that the drop should detach when the mass satisfies,

$$Mg_0 = 2\pi a\alpha. \tag{5.48}$$

This is Tate's law from 1864 [Tat64]. It provides a simple method for measurement of surface tension because the mass of a drop can be determined by weighing the liquid accumulated by many drops. There are of course corrections to this simple expression, the main being that only part of the liquid in a pendant drop actually detaches (see [YXB05]).

The mass of a drop can actually be determined from the balance of forces at $z = 0$,

$$Mg_0 = 2\pi a\alpha \sin\chi - \pi a^2 \Delta p_0. \tag{5.49}$$

On the left we have the weight of the drop and on the right the total force due to surface tension minus the force due to the pressure excess Δp_0 in the liquid at $z = 0$. In problem 5.4 it is shown that this is an exact relation, derivable from the differential equations. Notice that the inequality (5.47) corresponds to $\Delta p_0 > 0$, implying that the pressure should be above atmospheric at $z = 0$ for the inequality to hold. Tate's Law implies that the drop detaches when $\chi = 90°$ and the pressure excess vanishes, $\Delta p_0 = 0$.

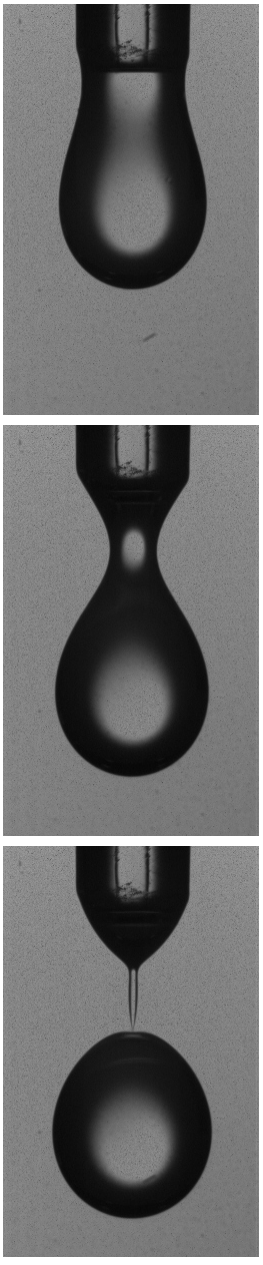

Slowly fed pendant drop. Images courtesy Anders Andersen, Technical University of Denmark. **Top:** Typical shape similar to the static ones in figure 5.10. **Middle:** Stretching the neck. **Bottom:** The moment of detachment.

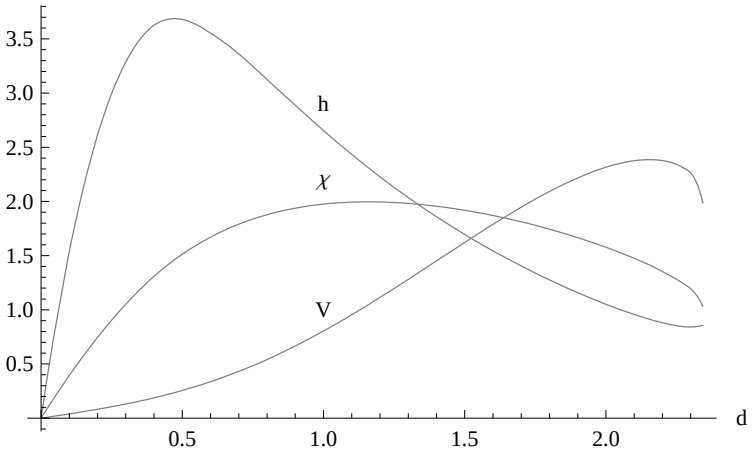

Figure 5.11. Drop parameters for the capillary with footprint radius $a = 0.5$ pictured in figure 5.10. All quantities are plotted in units where $L_c = 1$. Notice that the volume has a maximum as a function of depth at $d = 2.154\ldots$, which marks the limit to the static shapes that can be created by slowly feeding the drop through the capillary.

Numeric solution

The pressure excess in the liquid takes the same form as before

$$\Delta p = \rho_0 g_0 (h - z) \tag{5.50}$$

where $z = h$ is the height at which the liquid pressure equals the atmospheric. The solution of the three coupled first-order differential equations, (5.37) and (5.39) , proceeds as previously with the boundary conditions

$$r = 0, \qquad z = -d, \qquad \theta = 0 \qquad (s = 0), \tag{5.51a}$$
$$r = a, \qquad z = 0, \qquad \theta = \chi \qquad (s = s_0). \tag{5.51b}$$

Since there is no constraint on the angle χ, one may specify the depth d and the radius a, leaving h, χ and s_0 as unknowns.

In figure 5.10 two sets of solutions are shown for a capillary tubes with radii $a = 0.5$ and $a = 1.5$ in units where $L_c = 1$. The solution are parameterized by the depth d. The shapes with $d = 2.154\ldots$ and $d = 2.631\ldots$ are limiting cases, and although there are static solutions with larger values of d, they have smaller volumes and cannot be reached by feeding the drop through the tube. They must for this reason be unstable even if they are static. In figure 5.11 the parameters for the $a = 0.5$ set of pendant drop shapes are shown as a function of depth.

At $z = 0$ we have $\Delta p = \rho_0 g_0 h$, implying that we must have $h > 0$ to obtain the naive in equality (5.47) . This is in fact the case for all the shapes shown in figure 5.10 for $a = 0.5$, whereas the largest shape for $a = 1.5$ has $h = -0.27$, such that part of the drop's weight is carried by the negative pressure excess $z = 0$. Negative pressure excess, which by the Young-Laplace law is the same as negative mean curvature, can only occur if the first principal radius of curvature R_1 becomes negative at $z = 0$, which it is also seen to be the case in the figure.

Problems

5.1 A soap bubble of diameter 6 cm floats in air. What is the pressure excess inside the bubble when the surface tension between soapy water and air is taken to be $\alpha = 0.15\ \mathrm{N\ m^{-1}}$? How would you define the capillary length in this case, and how big is it? Do you expect the bubble to keep its spherical shape?

5.2 **(a)** Calculate the leading order change in area and volume of a column of incompressible fluid subject to an infinitesimal radial periodic perturbation with wavelength λ. **(b)** Show that the Rayleigh–Plateau stability condition is equivalent to the requirement that the area should grow for fixed volume. Instability occurs when the area diminishes.

* **5.3** Determine the radii of curvature in section 5.7 by expanding the shape $z = f(r)$ with $r = \sqrt{x^2 + y^2}$ to second order around $x = x_0$, $y = 0$, and $z = z_0$.

* **5.4** Show that the volume of a pendant droplet is $V = \int_{-d}^{0} \pi r^2\, dz = 2\pi a L_c^2 \sin\chi - \pi a^2 h$.

5.5 Show that eq. (5.45) can be derived from a simple model, just as in section 5.6.

5.6 Show that the condition that the condition for gravity on the air in a soap bubble to be negligible is that its radius satisfies $2a \ll h_0$ where $h_0 = p_0/\rho_0 g_0 \approx 8.4$ km is the scale height of the atmosphere.

5.7 Show that the radial component of gravity adds a correction to the difference in air pressure $\Delta p = p_{\text{inside}} - p_{\text{outside}}$

$$\Delta p = \frac{4\alpha}{R} + \rho_1 h g_0 \cos\theta \tag{5.52}$$

and estimate the size of the radial change.

5.8 Show that the Bond number (5.7) can be written as the ratio of the weight of the bubble and the force due to surface tension acting on its equator.

5.9 Calculate the size of the spherical drops that arise when a liquid column breaks up (assume that the fastest breakup yields one drop for each wavelength).

5.10 **(a)** Show that for a general curve $y = y(x)$ the radius of curvature is

$$\frac{1}{R} = \frac{y''(x)}{\left[1 + y'(x)^2\right]^{\frac{3}{2}}} \tag{5.53}$$

(b) Show that for a general curve $x = x(y)$ the radius of curvature is

$$\frac{1}{R} = -\frac{x''(y)}{\left[1 + x'(y)^2\right]^{\frac{3}{2}}} \tag{5.54}$$

5.11 Calculate the force per unit of length that the planar meniscus exerts on the vertical wall.

5.12 **(a)** Show that for a general curve $z = z(r)$ we have

$$\frac{1}{R_1} = \frac{z''(r)}{\left[1 + z'(r)^2\right]^{\frac{3}{2}}}, \qquad \frac{1}{R_2} = \frac{z'(r)}{r\sqrt{1 + z'(r)^2}} \tag{5.55}$$

(b) Show that for a general curve $r = r(z)$ we have

$$\frac{1}{R_1} = -\frac{r''(z)}{\left[1 + r'(z)^2\right]^{\frac{3}{2}}}, \qquad \frac{1}{R_2} = \frac{1}{r(z)\sqrt{1 + r'(z)^2}} \tag{5.56}$$

5.13 Consider the zero mean curvature soap film in figure 5.3a. Show that the shape is given by,

$$r = a \cosh \frac{z}{a} \tag{5.57}$$

with suitable choice of a and origin of z.

5.14 Assume that the pendant drop is spherical. Use Tate's law to obtain an approximate expression for its radius R when it detaches and falls.